



HAL
open science

Microwave Spectrum and Internal Rotations of Heptan-2-one: A Pheromone in the Gas Phase

Maike Andresen, Isabelle Kleiner, Martin Schwell, Wolfgang Stahl, Ha Vinh Lam Nguyen

► **To cite this version:**

Maike Andresen, Isabelle Kleiner, Martin Schwell, Wolfgang Stahl, Ha Vinh Lam Nguyen. Microwave Spectrum and Internal Rotations of Heptan-2-one: A Pheromone in the Gas Phase. *Journal of Physical Chemistry A*, 2020, 124 (7), pp.1353-1361. 10.1021/acs.jpca.9b11577 . hal-03182969

HAL Id: hal-03182969

<https://hal.u-pec.fr/hal-03182969>

Submitted on 12 Apr 2021

HAL is a multi-disciplinary open access archive for the deposit and dissemination of scientific research documents, whether they are published or not. The documents may come from teaching and research institutions in France or abroad, or from public or private research centers.

L'archive ouverte pluridisciplinaire **HAL**, est destinée au dépôt et à la diffusion de documents scientifiques de niveau recherche, publiés ou non, émanant des établissements d'enseignement et de recherche français ou étrangers, des laboratoires publics ou privés.

The Microwave Spectrum and Internal Rotations of Heptan-2-one: A Pheromone in the Gas-Phase

Maike Andresen,^{a,b} Isabelle Kleiner,^{b} Martin Schwell,^b Wolfgang Stahl^a and Ha Vinh Lam
Nguyen^b*

^a Institute of Physical Chemistry, RWTH Aachen University, Landoltweg 2, D-52074 Aachen,
Germany.

^b Laboratoire Interuniversitaire des Systèmes Atmosphériques (LISA), CNRS UMR 7583,
Université Paris-Est Créteil (UPEC), Université de Paris, Institute Pierre Simon Laplace, 61
avenue du Général de Gaulle, F-94010 Créteil, France.

ABSTRACT

The microwave spectrum of heptan-2-one ($\text{CH}_3\text{COC}_4\text{H}_8\text{CH}_3$) was recorded in the frequency range from 2 to 40 GHz using two molecular jet Fourier transform microwave spectrometers. The two energetically most favorable conformers could be identified and fitted with standard deviations close to measurement accuracy. The splittings arising from the internal rotations of two methyl groups, the acetyl methyl group $\text{CH}_3\text{CO-}$ and the pentyl methyl group $-\text{C}_4\text{H}_8\text{CH}_3$, could be resolved. The barrier to the internal rotation of the acetyl methyl group is $185.666(14) \text{ cm}^{-1}$ and $233.418(32) \text{ cm}^{-1}$ for conformer I and II, respectively, and can be linked to their specific geometries. For the pentyl methyl group, the respective barrier heights are $982.22(86) \text{ cm}^{-1}$ and $979.2(21) \text{ cm}^{-1}$.

INTRODUCTION

Heptan-2-one, also called methyl *n*-pentyl ketone, is a saturated methyl alkyl ketone. In nature, it acts as a pheromone. As early as 1965, heptan-2-one has been detected in the mandibular glands of honey bees.¹ Since then, it has been found to be a main component of the pheromone cocktail of several other bee species, which is often composed of a mixture of several tens to hundreds different compounds, i.a. alcohols, ketones, aldehydes, acids, and esters.²⁻⁴ Furthermore, heptan-2-one has also been identified as a pheromone component in many other animal classes, such as in the urine of mice.⁵

Pheromones are signal substances conveying information from one individual of a species to another. They exist within all animals and trigger behavioral changes. The effects and tasks of pheromones are numerous. Among others, they act as marker for food or territory, regulate social behavior, control the selection of partners, as well as trigger alarms and attacks.⁶ The first pheromone, which has been isolated and analyzed in 1959 by Butenandt *et al.*, was bombykol, a substance used by female silk moths (*Bombyx mori*) to attract males.⁷ Over decades, identification and extraction of pheromones have become much easier, however, the exact functional mechanisms of the pheromone-receptor interactions at a molecular level still remain veiled. As known so far, the famous “lock and key” model by Fisher turns out to be oversimplified.⁸ For example, receptors for one target substance may also accept other molecules, while multiple receptors designed to detect the same functional group have been observed to show quite different structures. It is also not possible to satisfactorily identify, whether the molecules are bonded to the receptors through a covalent, hydrogen, or van der Waals interaction.⁶

Though the composition of the pheromone mixture and the presence of certain functional groups play the most decisive role, an important aspect might also be the preference of a given receptor to a certain conformational structure of the pheromone substance. Fundamental knowledge about these gas-phase conformers may serve as a good starting point for further investigations. For this purpose, microwave spectroscopy is a useful tool, because it enables a clear distinction of conformational isomers close in energy. Some of many examples are the microwave spectroscopic studies on 1-heptanal,⁹ (*R*)-(+)-limonene oxide,¹⁰ propofol,¹¹ and α -D-galactose¹². In the studies on trifluoroacetone,¹³ acetyl acetone,¹⁴ and hexafluoroacetylacetone¹⁵ the two molecular versions of their keto-enol tautomerism could be distinguished.

In some of our previous works, we have successfully investigated the conformers of butan-2-one (**1**),¹⁶ pentan-2-one (**2**)¹⁷ and hexan-2-one (**3**)¹⁸ (for molecule numbering see Figure 1). Heptan-2-one (**4**) is the next member of this series of methyl *n*-alkyl ketones. In the present work, the complex conformational landscape and internal dynamics of heptan-2-one (**4**) are investigated using a combination of microwave spectroscopy and quantum chemistry. Moreover, the results are compared to current literature with the focus of interest on the effects of the internal rotation of the two terminal methyl groups.

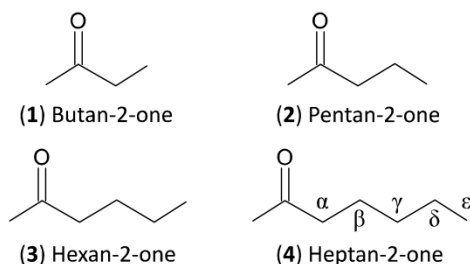


Figure 1. A series of methyl *n*-alkyl ketones.

QUANTUM CHEMICAL CALCULATIONS

Geometry Optimizations. Heptan-2-one is a medium-size molecule with a relatively long alkyl chain. Therefore, a large number of different conformational isomers are possible, which can be described by four dihedral angles, $\theta_1 = \angle(C_1, C_5, C_7, C_{10})$, $\theta_2 = \angle(C_5, C_7, C_{10}, C_{13})$, $\theta_3 = \angle(C_7, C_{10}, C_{13}, C_{16})$, and $\theta_4 = \angle(C_{10}, C_{13}, C_{16}, C_{19})$ (for atom numbering see Figure 2). The variation of the dihedral angles $\alpha_1 = \angle(H_2, C_1, C_5, C_7)$ and $\alpha_2 = \angle(C_{13}, C_{16}, C_{19}, H_{21})$ refers to the internal rotation of the acetyl methyl and the pentyl methyl group, respectively, and does not create different conformers. Each of the four angles θ_i ($i = 1-4$) was set to 180° , 60° and -60° , resulting in $3^4 = 81$ starting geometries. Under the experimental conditions described in the section *Microwave Spectrum*, we expected that only the energetically most favorable conformers are visible in the measured spectrum. Previous studies on pentan-2-one (**2**)¹⁷ and hexan-2-one (**3**)¹⁸ have shown that the energetically most favorable conformers of hexan-2-one (**3**) contain the energetically most favorable conformers of pentan-2-one (**2**) as sub-structures. Therefore, we extrapolate that the energetically most favorable conformers of heptan-2-one (**4**) contain the energetically most favorable conformers of hexan-2-one (**3**) as sub-structures, as well. Hence, the number of starting geometries could be reduced to 33, when the 11 conformers of hexan-2-one (**3**) reported in Ref. 18 were taken as starting points and only the additional dihedral angle θ_4 of heptan-2-one (**4**) was set to 180° , 60° and -60° .

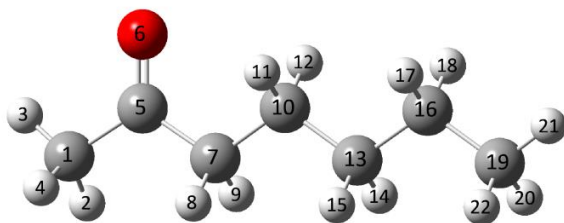


Figure 2. Atom numbering of heptan-2-one. The hydrogen atoms are white, the carbon atoms gray, and the oxygen atom is red.

With these 33 starting structures, geometry optimizations using the Gaussian09 package¹⁹ were performed. Calculations at the MP2/6-311++G(d,p) level of theory yielded 32 stable conformers and frequency calculations confirmed them to be true minima rather than saddle points. The above mentioned level was chosen due to its reasonable balance between speed of calculations and accuracy of the results, as can be seen in many previous studies.²⁰⁻²² Nevertheless, in the case of hexan-2-one (**3**),¹⁸ the B3LYP/6-311++G(d,p) level of theory has predicted a more reliable energetic order of the conformers. Therefore, the whole optimization procedure for heptan-2-one (**4**) was redone at the B3LYP/6-311++G(d,p) level, yielding 30 stable conformers. In this work, we focus on the two energetically most favorable conformers predicted with the B3LYP method, hereafter called conformer I and conformer II, which could eventually be identified in the microwave spectrum (see section *Spectral Assignment*). The two conformers are illustrated in Figure 3; their relative energies, rotational constants, dipole moment components, and optimized dihedral angles are collected in Table 1. The nuclear coordinates are given in Table S1 of the Supporting Information (SI).

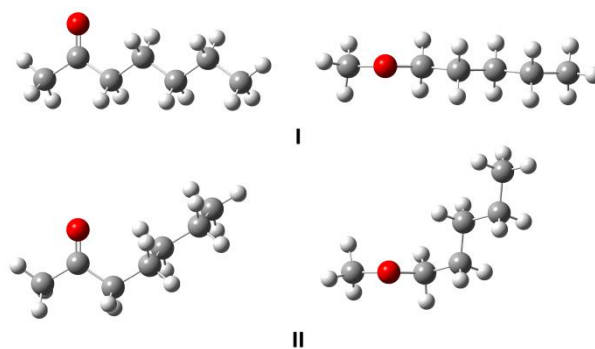


Figure 3. Geometries of the two assigned conformers of heptan-2-one optimized at the B3LYP/6-311++G(d,p) level of theory. Left hand side: view on the C–CO–C plane. Right hand side: view along the O=C bond.

Table 1. The rotational constants (in GHz), dipole moment components (in D), and optimized dihedral angles (in degree), as well as the relative equilibrium and zero-point corrected energies (in kJ mol^{-1}) of the two assigned conformers of heptan-2-one calculated at the MP2/6-311++G(d,p) and B3LYP/6-311++G(d,p) levels of theory.

| | Conformer I | | | Conformer II | | |
|------------------------|-------------------|-------------------|-------------------|-------------------|-------------------|-------------------|
| | MP2 | B3LYP | Exp. ^a | MP2 | B3LYP | Exp. ^a |
| <i>A</i> | 6.915 | 6.983 | 6.964 | 4.217 | 4.433 | 4.465 |
| <i>B</i> | 0.650 | 0.643 | 0.650 | 0.822 | 0.790 | 0.808 |
| <i>C</i> | 0.608 | 0.602 | 0.608 | 0.784 | 0.755 | 0.766 |
| $ \mu_a $ | 0.43 | 0.44 | | 0.80 | 0.67 | |
| $ \mu_b $ | 3.19 | 2.81 | | 2.05 | 2.04 | |
| $ \mu_c $ | 0.10 | 0.05 | | 2.29 | 1.81 | |
| θ_1 | 169.4 | -174.9 | | 161.5 | 165.9 | |
| θ_2 | 178.8 | -179.2 | | -70.3 | -73.0 | |
| θ_3 | 179.7 | 179.8 | | 179.0 | -180.0 | |
| θ_4 | 179.9 | -180.0 | | 179.5 | 179.7 | |
| <i>E</i> | 2.44 ^b | 0.00 ^c | | 0.00 ^b | 0.73 ^c | |
| <i>E_{ZPE}</i> | 1.64 ^d | 0.00 ^e | | 0.00 ^d | 1.19 ^e | |

^a Experimental rotational constants obtained from the *XIAM(1Top)* fits. ^b Relative to the absolute energy of $E = -349.439836$ Hartree of conformer II. ^c Relative to the absolute energy of $E = -350.515894$ Hartree of conformer I. ^d Relative to the zero-point corrected energy of $E_{ZPE} = -349.239778$ Hartree of conformer II. ^e Relative to the zero-point corrected energy of $E_{ZPE} = -350.319097$ Hartree of conformer I.

All heavy atoms of conformer I seem to lie in one plane and the molecular symmetry should be C_s . However, calculations with both, the MP2 and B3LYP methods, suggest that the entire *n*-pentyl chain is slightly tilted out of the C–CO–C plane by approximately 10° ($\theta_1 = 169.4^\circ$) and 5° ($\theta_1 = -174.9^\circ$), respectively. A conformer with such a tilt-distorted symmetry, hereafter called “pseudo- C_s ”, has been observed for all shorter alkyl methyl ketones (**1-3**)¹⁶⁻¹⁸ and some other ketones like diethyl ketone²³ and methyl neopentyl ketone.²⁴ This tilt-distorted symmetry will be further discussed in the section *Discussion*.

Conformer II shows a C_1 symmetry where the γ -carbon (C_{13}) of the alkyl chain (see Figure 1 and Figure 2) is in a nearly synclinal position. As expected, it contains the C_1 conformer of

pentan-2-one (**2**)¹⁷ and hexan-2-one (**3**)¹⁸ as a sub-structure. Similar observations have been found in a series of systematic microwave spectroscopic studies on *n*-alkyl acetates²⁵⁻³⁰ and methyl alkanoates.^{31,32}

Basis Set Variation. The very dense microwave spectrum of heptan-2-one, as will be presented in the section *Microwave Spectrum*, in combination with its rich conformational landscape requires precisely predicted rotational constants for a successful assignment. Unfortunately, results from the calculations at the MP2/6-311++G(d,p) and B3LYP/6-311++G(d,p) level of theory provide this quality only to a limited extent (see section *Spectral Assignment*). To find better alternatives, further geometry optimizations with the MP2,³³ B3LYP,³⁴ and B3PW91³⁵ methods in combination with different basis sets were carried out. Moreover, calculations with the Gaussian16 package³⁶ were also performed, using the M06-X2 method,³⁷ as well as the B3LYP functional including Grimme's dispersion correction without (DFT-D3)³⁸ or with Becke-Johnson damping (DFT-D3BJ).³⁹ The results for both conformers are listed in Table S2 and S3 of the SI and discussed in the section *Discussion*.

Internal Rotation. Heptan-2-one possesses two methyl groups undergoing internal rotation, the acetyl methyl group $\text{CH}_3\text{CO}-$ and the pentyl methyl group $-\text{C}_4\text{H}_8\text{CH}_3$, causing each rotational transition to split into a quintet of lines. The five torsional species are called $(\sigma_1\sigma_2) = (00), (01), (10), (11)$ and (12) , whereas σ_1 refers to the acetyl methyl and σ_2 to the pentyl methyl group. The designations $\sigma = 0, 1, 2$ represent the A, E_a, and E_b symmetry species of the C₃ group, respectively.⁴⁰

To determine the barriers to the internal rotation of the two methyl groups, the respective dihedral angles $\alpha_1 = \angle(\text{H}_2, \text{C}_1, \text{C}_5, \text{C}_7)$ and $\alpha_2 = \angle(\text{C}_{13}, \text{C}_{16}, \text{C}_{19}, \text{H}_{21})$ were each varied in a grid of 10°

increments, while all other parameters were optimized at the MP2/6-311++G(d,p) and the B3LYP/6-311++G(d,p) level. Because the symmetry of a methyl group is C_3 , a rotation of 120° was sufficient to describe its threefold potential curve. In a next step, the resulting energies were parameterized with a one-dimensional Fourier expansion. The corresponding Fourier coefficients are listed in Table S4 of the SI.

Acetyl Methyl Rotation. In case of conformer I, the potential energy curve, as illustrated in Figure 4, shows a significant V_6 contribution, and each of the three potential wells is divided by a local barrier into a pair of minima. For a closer look at this phenomenon, calculations at both, the MP2 and the B3LYP level, were repeated in a range of $\pm 20^\circ$ around a local maximum using a finer step width of 1° , (see the inset of Figure 4). The heights of the local barriers are 18.2 cm^{-1} and 1.0 cm^{-1} , respectively. The global barrier heights are 146.8 cm^{-1} (MP2) and 114.0 cm^{-1} (B3LYP). The two pits of a double minimum refer to the two enantiomers of conformer I. Upon the rotation of the acetyl methyl group, there is an oscillation motion of the entire *n*-pentyl group, changing between the enantiomeric structures, as depicted in the lower trace of Figure 4. This observation substantiates the “pseudo- C_s ” geometry of this conformer (see section *Geometry Optimizations*) and will be discussed in detail in the section *Discussion*.

In Figure 5 the respective potential energy curve of conformer II is given. Although, as expected, we observe a threefold potential with single minima, the potential shape is not entirely symmetric and higher order terms are necessary to parameterize the energy curve. In this case, there also is an oscillation of the entire *n*-pentyl group, now of about 17° (see the lower trace of Figure 5), which indicates a certain degree of flexibility of the alkyl chain about the C_5 - C_7 bond. The barriers to internal rotation predicted at the MP2 and B3LYP level are 228.3 cm^{-1} and 162.7 cm^{-1} , respectively.

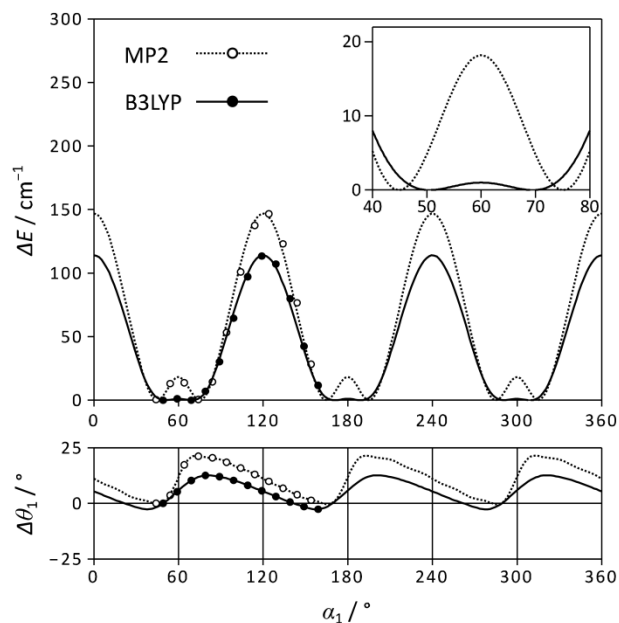


Figure 4. Upper trace: Potential energy curves obtained by rotating the acetyl methyl group of conformer I of heptan-2-one. The energies are calculated at the MP2/6-311++G(d,p) and B3LYP/6-311++G(d,p) level of theory and given relative to the lowest energy conformations with $E = -349.438905$ and -350.515894 Hartree, respectively. Inset: The double minimum between $\alpha_1 = 40^\circ$ and 80° depicted at an enlarged scale. Lower trace: Oscillation of the entire pentyl group upon the rotation of the acetyl methyl group. The deviations of the dihedral angle $\theta_1 = \angle(C_1, C_5, C_7, C_{10})$ are given relative to the values $\theta_1 = 169.4^\circ$ (MP2) and $\theta_1 = 174.9^\circ$ (B3LYP) of the fully optimized geometries.

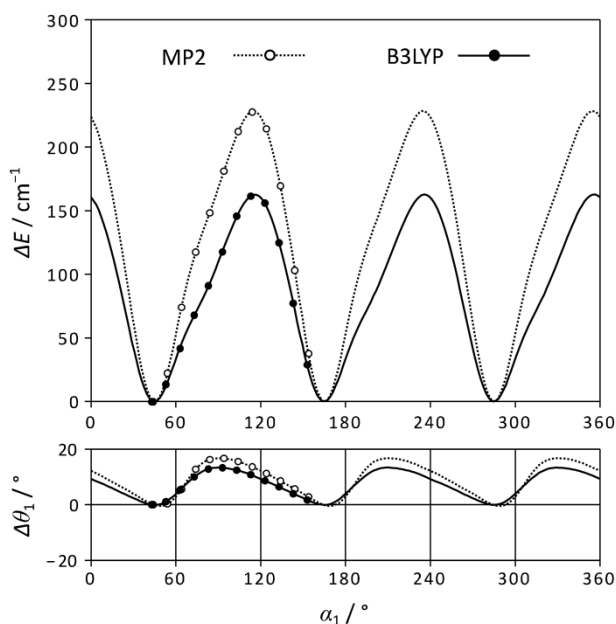


Figure 5. Upper trace: Potential energy curves obtained by rotating the acetyl methyl group of conformer II of heptan-2-one. The energies are calculated at the MP2/6-311++G(d,p) and B3LYP/6-311++G(d,p) level of theory and given relative to the lowest energy conformations with $E = -349.439836$ and -350.515618 Hartree, respectively. Lower trace: Oscillation of the entire pentyl group upon the rotation of the acetyl methyl group. The deviations of the dihedral angle $\theta_1 = \angle(\text{C}_1, \text{C}_5, \text{C}_7, \text{C}_{10})$ are given relative to the values $\theta_1 = 161.5^\circ$ (MP2) and $\theta_1 = 165.9^\circ$ (B3LYP) of the fully optimized geometries.

Pentyl Methyl Rotation. For the pentyl methyl group, the threefold curves of both conformers are of almost pure V_3 shape each and only very small contributions of higher order exist, as shown in Figure S1 in the SI. In case of conformer I, the barrier height predicted at the MP2 level is 1059.2 cm^{-1} , and 995.8 cm^{-1} with the B3LYP method. The respective values for conformer II are 1066.8 cm^{-1} and 999.6 cm^{-1} .

MICROWAVE SPECTRUM

Experimental Setup and Measurement Accuracy. The microwave spectrum of heptan-2-one was recorded using two molecular jet Fourier transform microwave spectrometers as described in Ref. 41 and 42, which cover a frequency range from 2 to 40 GHz. The substance was placed on a piece of a pipe cleaner. Helium at a pressure of about 200 kPa was allowed to flow over the sample and the helium-substance mixture was expanded into the Fabry-Perot resonator. Heptan-2-one was purchased from Alfa Aesar GmbH & Co KG, Karlsruhe, Germany, with a stated purity of 99 %, and no further purification steps were performed.

There are two operating modes of the spectrometers. First, a series of adjacent spectra in the so-called scan mode was measured from 9.7 to 13.7 GHz, as shown in Figure S2 in the SI, revealing a very dense spectrum, especially in the range of 9.7 to 12.2 GHz. Subsequently, measurements were performed in the high resolution mode for the scan region. After successful assignment, signals beyond the scan range were also recorded.

The chosen step width of 0.25 MHz decides the resolution of the broadband scan. The predicted barriers to the internal rotation of the acetyl methyl group range from about 100 cm^{-1} to 250 cm^{-1} (see section *Internal Rotation*). In the microwave spectrum of other methyl alkyl ketones, like butan-2-one (**1**),¹⁶ pentan-2-one (**2**)¹⁷ and hexan-2-one (**3**)¹⁸ this caused splittings into the (00) and (10) species of several MHz up to some GHz. Therefore, we expect splittings in the same order of magnitude for 2-heptanone (**4**), which are thus well-resolvable in the broadband scan.

Additionally, the internal rotation of the pentyl methyl group causes all (00) species lines to split into the (00) and (01) species, while all (10) species transitions split into (10), (11) and (12)

species lines. Quantum chemistry predicts barrier heights of about 1000 cm^{-1} for this methyl group (see section *Internal Rotation*), and our experiences from the microwave spectra of other methyl alkyl ketones (**1-3**) have shown that such a torsional barrier leads to splittings in the order of a few hundred down to less than 2 kHz.¹⁶⁻¹⁸ Those splittings are only resolvable in the high resolution mode. For heptan-2-one (**4**), about 30% of all transitions feature resolvable splittings. In case of the other 70%, a line broadening is observed. Consequently, the measurement accuracy of the heptan-2-one spectra is estimated to be approximately 3-4 kHz, while the instrumental accuracy achievable in the high-resolution mode is approximately 1 to 2 kHz.⁴³ In Figure 6 two typical high-resolution measurements of the $4_{22} \leftarrow 3_{13}$ transition of conformer II are given.

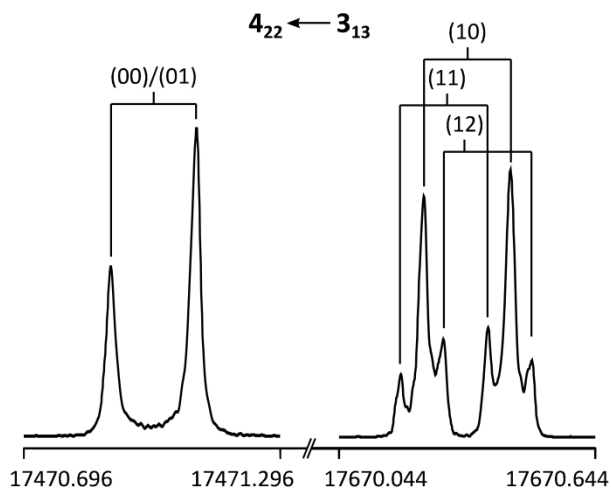


Figure 6. Two typical high resolution measurements of the $4_{22} \leftarrow 3_{13}$ transition of conformer II of heptan-2-one. The frequencies are in MHz. The (00), (10), (11) and (12) species are found at 17470.9960 MHz, 17670.3342 MHz, 17670.2907 MHz, and 17670.3867 MHz, respectively. The splitting between the (00) and (01) species is not resolvable. The brackets indicate the Doppler doublet.

Spectral Assignment

Conformer I (“pseudo- C_s ”). At the beginning, the internal rotations of both terminal methyl groups were neglected and the molecule was considered to be a rigid rotor. The rotational constants of conformer I calculated at the MP2/6-311++G(d,p) level of theory (see Table 1) were inserted as initial values in the *XIAM* program.⁴⁴ Despite the high density of the spectral lines (see section *Experimental Setup and Measurement Accuracy*), several *a*- and *b*-type transitions could be assigned after some cycles of trial and error. In a second step, the internal rotation of the acetyl methyl group was also taken into account. The initial angles between the internal rotor axis i_1 and the principal axes a , b , and c were obtained from calculations at the MP2/6-311++G(d,p) level, but it is noteworthy that in the final fit $\alpha(i_1, c)$ had to be fixed to 90° . For the potential barrier height of the acetyl methyl group, here called the $V_{3,1}$ potential, the starting value of 186.920 cm^{-1} was taken, which is the value found for the “pseudo- C_s ” conformer of hexan-2-one (**3**).¹⁸ Previous studies on pentan-2-one (**2**)¹⁷ and hexan-2-one (**3**)¹⁸ have shown that this value should be much more reliable than the values calculated at the MP2/6-311++G(d,p) or the B3LYP/6-311++G(d,p) level of theory (see section *Internal Rotation*).

Eventually, a total of 285 (00) and (10) species lines could be assigned to conformer I. The experimentally deduced parameters are listed in Table 2 as *XIAM(ITop)* fit with a root-mean-square (rms) deviation of 6.5 kHz, which is about twice the measurement accuracy (see section *Experimental Setup and Measurement Accuracy*). This elevated rms deviation is mainly caused by systematic deviations of certain branches, indicating that some higher order parameters are missing in the Hamiltonian.

To validate the *XIAM(1Top)* fit, the same data set of 285 lines was refitted using the *BELGI-Cs* code.⁴⁵ By floating 13 parameters, some of them belonging to higher order terms (see Table S5 of the SI), the rms deviation decreases to 3.5 kHz, a value in good agreement with the measurement accuracy. *BELGI* parameters which are transformable into the principal axis system are also given in Table 2. A list of all frequencies and their residuals is shown in Table S6 of the SI.

Table 2. Molecular parameters of conformer I and II of heptan-2-one obtained from the *XIAM* and *BELGI* codes. The *BELGI* and *XIAM(1Top)* fits include only the internal rotation of the acetyl methyl group. The *XIAM(2Tops)* fits contain the internal rotation of both methyl groups.

| Parameter ^a | Conformer I | | | Conformer II | | |
|-----------------------------------|-----------------------------------|-----------------|--------------------------|-----------------------------------|-----------------|--------------------------|
| | BELGI-C _s ^b | XIAM(1Top) | XIAM(2Tops) ^c | BELGI-C ₁ ^b | XIAM(1Top) | XIAM(2Tops) ^d |
| A / GHz | 6.95042(13) | 6.9638384(29) | 6.9638442(26) | 4.40251(56) | 4.4652469(10) | 4.4652475(12) |
| B / GHz | 0.650203(39) | 0.65009654(12) | 0.65009790(12) | 0.81073(15) | 0.80820856(15) | 0.80820880(18) |
| C / GHz | 0.6086448(25) | 0.608408524(68) | 0.608406889(69) | 0.76739(10) | 0.766226397(75) | 0.766226085(87) |
| Δ_J / kHz | 0.0142(02) | 0.01363(30) | 0.01336(29) | | 0.16654(22) | 0.16655(25) |
| Δ_{JK} / kHz | | 0.2863(23) | 0.2829(23) | | -2.6595(21) | -2.6605(23) |
| Δ_K / kHz | | 4.301(36) | 4.346(32) | | 28.047(24) | 28.083(25) |
| δ_J / kHz | | 0.00087(11) | 0.00070(11) | | 0.012423(62) | 0.012438(73) |
| δ_K / kHz | | | | | 0.943(17) | 0.935(20) |
| $F_{0,1}$ / GHz | 158.578(40) | 158.0(fixed) | 158.0(fixed) | 166.40(43) | 158.0(fixed) | 158.0(fixed) |
| $V_{3,1}$ / cm ⁻¹ | 185.275(11) | 185.469(16) | 185.666(14) | 229.14(16) | 233.380(28) | 233.418(32) |
| $\chi(i_1,a)$ / ° | 34.551(15) | 34.770(18) | 34.820(15) | 29.714(96) | 29.739(37) | 29.764(42) |
| $\chi(i_1,b)$ / ° | 124.551(15) | 124.770(18) | 124.820(15) | 97.514(56) | 97.62(24) | 97.78(27) |
| $\chi(i_1,c)$ / ° | 90.00(fixed) | 90.00(fixed) | 90.00(fixed) | 118.56(10) | 118.55(11) | 118.53(12) |
| $D_{pi2,1}$ / MHz | | 0.01728(23) | 0.01774(22) | | 0.16066(41) | 0.16084(46) |
| $D_{pi2K,1}$ / MHz | | -0.976(12) | -1.010(12) | | -3.8902(78) | -3.8978(88) |
| $D_{pi2-,1}$ / MHz | | 0.003681(93) | 0.003820(93) | | 0.03973(17) | 0.03958(20) |
| $V_{3,2}$ / cm ⁻¹ | | | 982.22(86) | | | 979.2(21) ^b |
| $N(\text{total})^e$ | 285 | 285 | 406 | 448 | 448 | 545 |
| $N((00)/(10))^f$ | 145/140 | 145/140 | 145/140 | 262/186 | 262/186 | 262/186 |
| $N((01)/(11)/(12))^f$ | | | 22/47/52 | | | 15/41/41 |
| σ_{rms} / kHz ^g | 3.5 | 6.5 | 7.1 | 2.3 | 5.9 | 7.0 |

^a All parameters refer to the principal axis system. [†] representation and Watson's A reduction was used. ^b Parameters of the *BELGI* fits were transformed from the rho axis system into the principal axis system. ^c For conformer I, the internal rotation parameters of the second rotor are fixed to $F_{0,2} = 158.0$ GHz, $\chi(i_2,a) = 150.52^\circ$, $\chi(i_2,b) = 119.48^\circ$, and $\chi(i_2,c) = 90.00^\circ$. ^d For conformer II, they are $F_{0,2} = 158.0$ GHz, $\chi(i_2,a) = 128.17^\circ$, $\chi(i_2,b) = 128.59^\circ$, and $\chi(i_2,c) = 118.60^\circ$. ^e Total number of lines. ^f Number of the respective torsional species. ^g Root-mean-square deviation of the fit.

Conformer II (C_1). Following the same general strategy as for conformer I, conformer II could be identified and fitted. Nevertheless, using the rotational constants calculated at the MP2/6-311++G(d,p) or B3LYP/6-311++G(d,p) level of theory (see Table 1) did not result in sufficiently precise predictions for a successful assignment. This problem also occurred in other methyl alkyl ketones, such as hexan-2-one (**3**), where a discrepancy between the experimentally deduced and calculated constants of up to 5% has been observed.¹⁸ Assuming the same error compensation in geometry optimization calculations of hexan-2-one (**3**) and heptan-2-one (**4**), the deviations ΔX between the predicted and the experimental rotational constants ($X = A, B,$ and C) relative to the experimental values (in percent) should be similar for both molecules. Thus, we could deduce “guessed” rotational constants of heptan-2-one (**4**) using the following relation:

$$X_{guess} = (X_{cal} \cdot 100) / (\Delta X_{hexan-2-one} + 100) \quad (1).$$

Finally, the “guessed” values turned out to be very accurate. The barrier to the internal rotation of the acetyl methyl group observed for the C_1 conformer of hexan-2-one (**3**) is 233.5913 cm^{-1} ,¹⁸ and for the same reason as stated in section *Conformer I*, this barrier was taken as initial value for this parameter of heptan-2-one (**4**). The final *XIAM(1Top)* fit includes 448 lines and shows an rms deviation of 5.9 kHz. The *BELGI-C₁* code⁴⁶ decreases this value to 2.3 kHz by fitting 16 parameters. The molecular parameters are summarized in Table 2 and Table S5 in the SI, all assigned frequencies are listed in Table S7 of the SI.

Two-Top Fits. To include the internal rotation of the pentyl methyl group, resolvable transitions of the (01), (11), and (12) species were added to the *XIAM(1Top)* fits described in the preceding sections. The parameters of these new fits, which we call *XIAM(2Tops)*, are also stated in Table 2. The total number of lines increases to 406 and 545 for conformer I and II,

respectively, while the rms deviations are 7.1 kHz and 7.0 kHz. If only $V_{3,2}$ and the (01), (11), and (12) species lines are fitted, whereas the line positions are considered relative to that of their respective (00) and (10) transition, the rms deviation decreases to 3.7 kHz for conformer I and 4.9 kHz for conformer II. The fitted frequencies are given in Table S8 and S9 in the SI.

DISCUSSION

Geometry Parameters. The microwave spectra of conformer I and conformer II of heptan-2-one were assigned and fitted to measurement accuracy. The parameters obtained from the *XIAM* fits agree with the *BELGI* values within 1%, but not within their standard errors. These discrepancies can be traced back to the use of certain higher order parameters in the *BELGI* fits to treat branches that are not properly reproduced with *XIAM* (see section *Spectral Assignment*).

If the experimentally deduced rotational constants are compared with the rotational constants calculated at different levels of theory (see section *Basis Set Variation*), the values are in good agreement for conformer I (within 1% or less). For conformer II, however, the constants coincide less, especially the *A* rotational constants calculated at certain MP2 levels, where the experimental and theoretical values differ up to 5%. This has also been observed for other linear methyl alkyl ketones (**1-3**),¹⁶⁻¹⁸ suggesting that some kind of interactions in this type of molecules are not correctly captured at those levels. The best calculation-experiment agreements (within 0.5 %) are found for Grimme's dispersion calculations in combination with polarization function while excluding diffuse functions. Hence, dispersion might be an important effect to be considered due to the relative long carbon chain of heptan-2-one (**4**). Nevertheless, a good agreement might just be explained by error compensation. The inaccurately calculated rotational constants cause more problems, if the line density of the experimental spectrum is very high, as it

is the case in this work (see section *Microwave Spectrum*), since then reliable predictions of the rotational constants are even more crucial for a successful assignment. Using Equation (1) to obtain the “guessed” rotational constants for the assignment of conformer II is essentially a calibration to correct the errors of a certain level of theory. Although such a calibration has led to convincing results while going from pentan-2-one (**2**)¹⁷ to hexan-2-one (**3**)¹⁸ and on to heptan-2-one (**4**) (this work), the application is very limited, since every different set of substance class, conformer, rotational constant and level of theory in use would need its own calibration. An alternative way to circumvent this problem is the modulation and analysis of line intensities using the strong field coherence breaking (SFCB) method, as has been applied by Fritz *et al.* for the chirped-pulse microwave spectrum of hexan-2-one (**3**).⁴⁷ There, it has led to the assignment of three conformers, similar to our own results investigating hexan-2-one (**3**) by using the calibration method.¹⁸

The experimental spectra of the C_s and the C₁ conformer are very similar in intensity. The comparable *a*- and *b*-dipole moment components predicted from quantum chemistry suggest a population ratio of approximately 1:1. However, a quantitative statement on the conformational intensity and stability is not attempted due to the lack of dipole moment measurements and the absence of trust in both, calculated dipole moments and intensity ratio obtained from the experimental setup. A chirped pulse spectrum⁴⁸ of heptan-2-one would be helpful to access more reliable intensity for quantitative comparison.

After the assignment of conformer I and conformer II, several lines of medium and weak intensity still remain in the microwave spectrum of heptan-2-one (see Figure S2 in the SI). These signals might arise from impurities, but also from one or several conformers, which are higher in energy. However, we were not able to find another assignment. Quantum chemistry yielded up to

15 conformers as possible candidates, all close in energy. Depending on the level of theory employed, the type and energy order of the conformers varies strongly. Additionally, the above mentioned problem of unprecise predictions of the calculated rotational constants observed for conformer II might appear for the higher energy conformers, as well. Moreover, the strongest lines of these conformers are expected to appear in the frequency region from 9 to 12 GHz, where the spectra of conformer I and II are very dense and might mask many signals of the less abundant conformers. Finally, several conformers other than conformer I and II probably exist simultaneously in the spectrum, each of them with only a few strong lines. Consequently, there are not enough lines belonging to one conformer left, to verify any assignment attempt.

Acetyl Methyl Rotation. Concerning the internal rotation of the acetyl methyl group, our recent studies on pentan-2-one (**2**)¹⁷ and hexan-2-one (**3**)¹⁸ propose a link between the barrier height of this torsion and the structural environment at the other side of the carbonyl group. Apparently, there are two classes of ketones containing an acetyl methyl group. The ketones of the first class always show a barrier height of approximately 240 cm⁻¹ and a characteristic bent geometry with C₁ symmetry, thus called the “C₁ class”. Examples are the C₁ conformer of pentan-2-one (**2**) (238.145(21) cm⁻¹),¹⁷ the C₁ conformer of hexan-2-one (**3**) (233.5913(97) cm⁻¹),¹⁸ methyl isobutyl ketone (250.3(19) cm⁻¹)⁴⁹ and allyl acetone (224.95(12) cm⁻¹).⁵⁰ Conformer II of heptan-2-one (**4**) with its barrier height of 233.380(28) cm⁻¹ (see *XIAM(1Top)* fit), where the γ -carbon atom of the pentyl group is bent to a nearly synclinal position (see section *Geometry Optimizations*), belongs to this class as well.

The second class encloses molecules like butan-2-one (**1**) (183.1702(89) cm⁻¹),¹⁶ the C_s conformer of pentan-2-one (**2**) (188.3843(50) cm⁻¹),¹⁷ the C_s conformer of hexan-2-one (**3**) (186.9198(50) cm⁻¹),¹⁸ methyl neopentyl ketone (173.539(36) cm⁻¹)²⁴ and cat ketone

(178.9706(19) cm⁻¹).⁵¹ For all of these ketones the barrier height is about 180 cm⁻¹ and a “pseudo-C_s” structure is observed. Hence, we call this the “C_s class”, which also comprises conformer I of heptan-2-one (**4**) with a torsional barrier of 185.469(16) cm⁻¹ (according to the *XIAM(1Top)* fit).

The “pseudo-C_s” structures observed for the latter class are interesting to discuss. As described in the section *Quantum Chemical Calculations*, all heavy atoms of conformer I of heptan-2-one seem to lie in a C_s symmetry plane, but calculations at the MP2/6-311++G(d,p), B3LYP/6-311++G(d,p), and many other levels of theory yield a structure with the entire *n*-pentyl group tilted out of this plane by up to 10°, leading to a double minimum in the potential energy curve of the acetyl methyl group (see Figure 4). Interestingly, conformer I of heptan-2-one (**4**), and all the other examples of the C_s class, while showing “pseudo-C_s” geometries in the calculations, were fitted with the *XIAM* and *BELGI* programs as “true C_s” molecules, i.e. $\chi(i_1, c) = 90^\circ$, use of the *BELGI-C_s* code, and no measurement of *c*-type transitions (see section *Spectral Assignment*). We note that the presence of a “pseudo-C_s” geometry is firmly linked to a barrier height of about 180 cm⁻¹, and that there are three possibilities for the real structure: (i) The symmetry of the conformer is C_s and the calculations fail to reproduce that correctly. (ii) The calculated “pseudo-C_s” geometry is correct, but the dipole moment component in *c*-direction is too small, so that *c*-type transitions are not observable in the spectrum. And (iii) the two enantiomers of the “pseudo-C_s” structure are only separated by a small barrier and the zero point energy of the tunneling ground state lies above this barrier, thus leading to an *effective* C_s structure.

There are also examples of molecules matching neither the C₁ nor the C_s class. Acetone, the smallest methyl alkyl ketone, does not fit because of two acetyl methyl groups undergoing coupled internal rotations.⁵² Moreover, molecules featuring mesomeric effects, such as methyl

vinyl ketone⁵³ and ionone,⁵⁴ or ring containing molecules like i.a. cyclopropyl methyl ketone,⁵⁵ 2-acetyl-5-methylfuran,⁵⁶ phenylacetone,⁵⁷ acetovanillone, and 6-hydroxy-3-methoxyacetophenone⁵⁸ show the acetyl methyl barrier to be up to about 620 cm⁻¹. Future studies to validate and expand this two-class concept will thus be necessary. Nevertheless, our results found for heptan-2-one strongly support the classification made for the other aliphatic methyl alkyl ketones of the series.

Pentyl Methyl Rotation. The calculated barrier to the internal rotation of the pentyl methyl group is approximately 1000 cm⁻¹ (see section *Internal Rotation*), which is in good agreement with the experimentally deduced barriers of 982.22(86) cm⁻¹ for conformer I and 979.2(21) cm⁻¹ for conformer II. In general, all parameters of the *XIAM(2Tops)* fits coincide with those of the *XIAM(1Top)* fits (see Table 2). However, the rms deviations of the former are about 1 kHz higher for both conformers, because (i) the signals of the (01), (11), and (12) transitions show overall weaker intensities than the (00) and (10) ones, thereby reducing the achievable frequency accuracy, and (ii) among the 15 parameters used in the *XIAM(2Tops)* fits, only the potential barrier $V_{3,2}$ accounts for the splittings caused by the pentyl methyl rotor. In the relative fits, where only the pentyl methyl torsional splittings are fitted instead of the absolute frequencies, the rms deviation decreases to almost measurement accuracy. Moreover, $V_{3,2}$ is determined more precisely with values of 980.81(25) cm⁻¹ and 979.72(64) cm⁻¹ for conformer I and conformer II, respectively.

CONCLUSIONS

The two energetically most favorable conformers of heptan-2-one were identified in the microwave spectrum and fitted to rms deviations close to measurement accuracy. The geometry

of conformer I is C_s or “pseudo- C_s ”, while conformer II features a C_1 structure with the γ -carbon of the *n*-pentyl chain bent to a nearly synclinal position. The torsional barrier of the acetyl methyl group is $185.666(14) \text{ cm}^{-1}$ for the former and $233.418(32) \text{ cm}^{-1}$ for the latter. Similar to the cases of other methyl alkyl ketones, such as butan-2-one (**1**),¹⁶ pentan-2-one (**2**)¹⁷ and hexan-2-one (**3**),¹⁸ these barrier heights can be linked to the respective conformational structures, confirming the observations found in previous studies of the series. Splittings arising from the internal rotation of the pentyl methyl group could also be resolved, yielding a barrier height of $982.22(86) \text{ cm}^{-1}$ and $979.2(21) \text{ cm}^{-1}$ for conformer I and II, respectively.

ASSOCIATED CONTENT

Supporting Information. Nuclear coordinates of the conformers in the principal axis system, basis set variation, Fourier coefficients of potential energy curves, survey spectrum, spectroscopic constants of the BELGI fits in the rho axis system, frequency lists.

AUTHOR INFORMATION

Corresponding Author

*Isabelle Kleiner, isabelle.kleiner@lisa.u-pec.fr

Author Contributions

The manuscript was written through contributions of all authors. All authors have given approval to the final version of the manuscript.

ACKNOWLEDGMENT

We thank Franziska Pfeiffer for her contributions to this paper during her student research project at the RWTH Aachen University. Simulations were performed with computing resources granted by RWTH Aachen University under project rwth0249. The DIM Q² is gratefully acknowledged for supporting the organization of the Journées de Spectroscopie Moleculaire (JSM) in Créteil where M. Andresen contributed a talk with the results.

Funding Sources

This work was supported by the Agence Nationale de la Recherche ANR (project ID ANR-18-CE29-0011).

REFERENCES

- (1) Shearer, D. A.; Boch, R. 2-Heptanone in the Mandibular Gland Secretion of the Honey-Bee. *Nature* **1965**, *206*, 530.
- (2) Francke, W.; Lübke, G.; Schröder, W.; Reckziegel, A.; Imperatriz-Fonseca, V.; Kleinert, A.; Engels, E.; Hartfelder, K.; Radtke, R.; Engels, W. Identification of Oxygen Containing Volatiles in Cephalic Secretions of Workers of Brazilian Stingless Bees. *J. Braz. Chem. Soc.* **2000**, *11*, 562-571.
- (3) Wittmann, D.; Lübke, G.; Francke, W. Cephalic Volatiles Identified in Workers of *Mourella caerulea*, a Rare Stingless Bee Recently Rediscovered in Southern Brazil. *Z. Naturforsch.* **1989**, *44c*, 325-326.

- (4) Boch, R.; Shearer, D. A. Chemical Releasers of Alarm Behaviour in the Honey-Bee, *Apis Mellifera*. *J. Insect. Physiol.* **1971**, *17*, 2277-2285.
- (5) Schaefer, M. L.; Wongravee, K.; Holmboe, M. E.; Heinrich, N. M.; Dixon, S. J.; Zeskind, J. E.; Kulaga, H. M.; Brereton, R. G.; Reed, R. R.; Trevejo, J. M. Mouse Urinary Biomarkers Provide Signatures of Maturation, Diet, Stress Level and Diurnal Rhythm. *Chem. Senses* **2010**, *35*, 459-471.
- (6) Bestmann, H. J.; Vostrowsky, O. Chemische Informationssysteme der Natur: Insektenpheromone. *Chem. unserer Zeit* **1993**, *27*, 123-133.
- (7) Butenandt, A.; Beckmann, R.; Stamm, D.; Hecker, E. Über den Sexual-Lockstoff des Seidenspinners *Bombyx Mori*. Reindarstellung und Konstitution. *Z. Naturforsch.* **1959**, *14b*, 283-284.
- (8) Fischer, E. Einfluss der Configuration auf die Wirkung der Enzyme. *Ber. d. Dt. Chem. Ges.* **1894**, *27*, 2985-2993.
- (9) Fisher, J. M.; Xu, L.-H.; Suenram, R. D.; Pate, B.; Douglass, K. Conformational Isomerism in 1-Heptanal. *J. Mol. Struct.* **2006**, *795*, 143-154.
- (10) Loru, D.; Quesada-Moreno, M. M.; Avilés-Moreno, J. R.; Jarman, N.; Huet, T. R.; López-González, J. J.; Sanz, M. E. Conformational Flexibility of Limonene Oxide Studied by Microwave Spectroscopy. *ChemPhysChem* **2017**, *18*, 274-280.

- (11) Lesarri, A.; Shipman, S. T.; Neill, J. L.; Brown, G. G.; Suenram, R. D.; Kang, L.; Caminati, W.; Pate, B. H. Interplay of Phenol and Isopropyl Isomerism in Propofol from Broadband Chirped-Pulse Microwave Spectroscopy. *J. Am. Chem. Soc.* **2010**, *132*, 13417-13424.
- (12) Peña, I.; Cabezas C.; Alonso, J. L.; Unveiling Epimerization Effects: a Rotational Study of α -D-Galactose. *Chem. Commun.* **2015**, *51*, 10115-10118.
- (13) Evangelisti, L.; Favero, L. B.; Maris, A.; Melandri, S.; Vega-Toribio, A.; Lesarri, A.; Caminati, W. Rotational Spectrum of Trifluoroacetone. *J. Mol. Spectrosc.* **2010**, *259*, 65-69.
- (14) Caminati, W.; Grabow, J.-U. The C_{2v} Structure of Enolic Acetylacetone. *J. Am. Chem. Soc.* **2006**, *128*, 854-857.
- (15) Evangelisti, L.; Tang, S.; Velino, B.; Giuliano, B. M.; Melandri, S.; Caminati, W. Hexafluoroacetylacetone: a 'Rigid' Molecule with an Enolic C_s Shape. *Chem. Phys. Lett.* **2009**, *473*, 247-250.
- (16) Nguyen, H. V. L.; Van, V.; Stahl, W.; Kleiner, I. The Effects of Two Internal Rotations in the Microwave Spectrum of Ethyl Methyl Ketone. *J. Chem. Phys.* **2014**, *140*, 214303.
- (17) Andresen, M.; Kleiner, I.; Schwell, M.; Stahl, W.; Nguyen, H. V. L. Acetyl Methyl Torsion in Pentan-2-one as Observed by Microwave Spectroscopy. *J. Phys. Chem. A* **2018**, *122*, 7071-7078.
- (18) Andresen, M.; Kleiner, I.; Schwell, M.; Stahl, W.; Nguyen, H. V. L. Sensing the Molecular Structures of Hexan-2-one by Internal Rotation and Microwave Spectroscopy *ChemPhysChem* **2019**, *20*, 2063-2073.

- (19) Frisch, M. J.; Trucks, G. W.; Schlegel, H. B.; Scuseria, G. E.; Robb, M. A.; Cheeseman, J. R.; Scalmani, G.; Barone, V.; Mennucci, B.; Petersson, G. A.; et al. *Gaussian 09, Revision A.02*, Gaussian, Inc., Wallingford CT **2009**.
- (20) Ottaviani, P.; Velino, B.; Caminati, W. Jet Cooled Rotational Spectrum of Methyl Lactate. *Chem. Phys. Lett.* **2006**, *428*, 236-240.
- (21) Van, V.; Stahl, W.; Schwell, M.; Nguyen, H. V. L. Gas-Phase Conformations of 2-Methyl-1,3-dithiolane Investigated by Microwave Spectroscopy. *J. Mol. Struct.* **2018**, *1156*, 348-352.
- (22) Van, V.; Bruckhuisen, J.; Stahl, W.; Ilyushin, V.; Nguyen, H. V. L. The Torsional Barriers of Two Equivalent Methyl Internal Rotations in 2-5-Dimethylfuran Investigated by Microwave Spectroscopy. *J. Mol. Spectrosc.* **2018**, *343*, 121-125.
- (23) Nguyen; H. V. L.; Stahl, W. The Rotational Spectrum of Diethyl Ketone *ChemPhysChem* **2011**, *12*, 1900-1905.
- (24) Zhao, Y.; Jin, J.; Stahl, W.; Kleiner, I. The Microwave Spectrum of Methyl Neopentyl Ketone. *J. Mol. Spectrosc.* **2012**, *281*, 4-8.
- (25) Tudorie, M.; Kleiner, I.; Hougen, J. T.; Melandri, S.; Sutikdja, L. W.; Stahl, W. A Fitting Program for Molecules with Two Inequivalent Methyl Tops and a Plane of Symmetry at Equilibrium: Application to New Microwave and Millimeter-Wave Measurements of Methyl Acetate, *J. Mol. Spectrosc.* **2011**, *269*, 211-225.

- (26) Jelisavac, D.; Cortés Gómez, D. C.; Nguyen, H. V. L.; Sutikdja, L. W.; Stahl, W.; Kleiner, I. The Microwave Spectrum of the *Trans* Conformer of Ethyl Acetate. *J. Mol. Spectrosc.* **2009**, *257*, 111-115.
- (27) Sutikdja, L. W.; Stahl, W.; Sironneau, V.; Nguyen, H. V. L.; Kleiner, I. Structure and Internal Dynamics of *n*-Propyl Acetate Studied by Microwave Spectroscopy and Quantum Chemistry. *Chem. Phys. Lett.* **2016**, *663*, 145-149.
- (28) Attig, T.; Sutikdja, L. W.; Kannengießer, R.; Kleiner, I.; Stahl, W. The Microwave Spectrum of *n*-Butyl Acetate. *J. Mol. Spectrosc.* **2013**, 284-285, 8-15.
- (29) Attig, T.; Kannengießer, R.; Kleiner, I.; Stahl, W. Conformational Analysis of *n*-Pentyl Acetate Using Microwave Spectroscopy. *J. Mol. Spectrosc.* **2013**, *290*, 24-30.
- (30) Attig, T.; Kannengießer, R.; Kleiner, I.; Stahl, W. The Microwave Spectrum of *n*-Hexyl Acetate and Structural Aspects of *n*-Alkyl Acetates. *J. Mol. Spectrosc.* **2014**, *298*, 47-53.
- (31) Nguyen, H. V. L.; Stahl, W.; Kleiner, I. Structure and Rotational Dynamics of Methyl Propionate Studied by Microwave Spectroscopy. *Mol. Phys.* **2012**, *110*, 2035-2042.
- (32) Hernandez-Castillo, A. O.; Abeysekera, C.; Hays, B. M.; Kleiner, I.; Nguyen, H. V. L.; Zwier, T. S. Conformational Preferences and Internal Rotation of Methyl Butyrate by Microwave Spectroscopy. *J. Mol. Spectrosc.* **2017**, *337*, 51-58.
- (33) Head-Gordon, M.; Head-Gordon, T. Analytic MP2 Frequencies without Fifth-Order Storage. Theory and Application to Bifurcated Hydrogen Bonds in the Water Hexamer. *Chem. Phys. Lett.* **1994**, *220*, 122-128.

- (34) Stephens, P. J.; Devlin, F. J.; Chabalowski, C. F.; Frisch, M. J. *Ab Initio* Calculation of Vibrational Absorption and Circular Dichroism Spectra Using Density Functional Force Fields. *J. Phys. Chem.* **1994**, *98*, 11623-11627.
- (35) Becke, A. D. Density-Functional Thermochemistry. III. The Role of Exact Exchange. *J. Chem. Phys.*, **1993**, *98*, 5648-5652.
- (36) . Frisch, M. J; Trucks, G. W.; Schlegel, H. B.; Scuseria, G. E.; Robb, M. A.; Cheeseman, J. R.; Scalmani, G.; Barone, V.; Petersson, G. A.; Nakatsuji, H.; et al. *Gaussian 16, Revision B.01*, Gaussian, Inc., Wallingford CT, **2016**.
- (37) Zhao, Y.; Truhlar, D. G. The M06 Suite of Density Functionals for Main Group Thermochemistry, Thermochemical Kinetics, Noncovalent Interactions, Excited States, and Transition Elements: Two New Functionals and Systematic Testing of Four M06-Class Functionals and 12 Other Functionals. *Theor. Chem Acc.* **2008**, *120*, 215-241.
- (38) Grimme, S.; Antony, J.; Ehrlich, S.; Krieg, H. A Consistent and Accurate *ab initio* Parametrization of Density Functional Dispersion Correction (DFT-D) for the 94 Elements H-Pu. *J. Chem. Phys.* **2010**, *132*, 154104.
- (39) Grimme, S.; Ehrlich, S.; Goerigk L. Effect of the Damping Function in Dispersion Corrected Density Functional Theory. *J. Comp. Chem.* **2011**, *32*, 1456-1465.
- (40) Dreizler, H. Gruppentheoretische Betrachtungen zu den Mikrowellenspektren von Molekülen mit zwei behindert drehbaren dreizählig-symmetrischen Molekülgruppen. *Z. Naturforsch.* **1961**, *16a*, 1354-1367.

- (41) Grabow, J.-U.; Stahl, W.; Dreizler, H. A Multioctave Coaxially Oriented Beam-Resonator Arrangement Fourier-Transform Microwave Spectrometer. *Rev. Sci Instrum.* **1996**, *67*, 4072-4084.
- (42) Merke, I.; Stahl, W.; Dreizler, H. A Molecular Beam Fourier Transform Microwave Spectrometer in the Range 26.5 to 40 GHz. Tests of Performance and Analysis of the D- and ¹⁴N-Hyperfine Structure of Methylcyanide-d₁. *Z. Naturforsch.* **1994**, *49a*, 490-496.
- (43) Garbow, J.-U.; Stahl, W. A Pulsed Molecular Beam Microwave Fourier Transform Spectrometer with Parallel Molecular Beam and Resonator Axes. *Z. Naturforsch.* **1990**, *45a*, 1043-1044.
- (44) Hartwig, H.; Dreizler, H. The Microwave Spectrum of Trans-2,3-Dimethyloxirane in Torsional Excited States. *Z. Naturforsch.* **1996**, *51a*, 923-932.
- (45) Hougen, J. T.; Kleiner, I.; Godefroid, M. Selection Rules and Intensity Calculations for a C_s Asymmetric Top Molecule Containing a Methyl Group Internal Rotor. *J. Mol. Spectrosc.* **1994**, *163*, 559-586.
- (46) Kleiner, I.; Hougen, J. T. Rho-Axis-Method Hamiltonian for Molecules Having One Methyl Rotor and C₁ Point-Group Symmetry at Equilibrium. *J. Chem. Phys.* **2003**, *119*, 5505-5509.
- (47) Fritz, S. M.; Mishra, P.; Zwier, T. S. Strong-Field Coherence Breaking as a Tool for Identifying Methyl Rotor States in Microwave Spectra: 2-Hexanone. *J. Chem. Phys.* **2019**, *151*, 041104.

- (48) Brown, G.G.; Dian, B.C.; Douglass, K.O.; Geyer, S.M.; Shipman, S.T.; Pate, B.H. A Broadband Fourier Transform Microwave Spectrometer Based on Chirped Pulse Excitation. *Rev. Sci. Instrum.* **2008**, *79*, 053103.
- (49) Zhao, Y.; Stahl, W.; Nguyen, H. V. L. Ketone Physics – Structure, Conformations, and Dynamics of Methyl Isobutyl Ketone Explored by Microwave Spectroscopy and Quantum Chemical Calculations. *Chem. Phys. Lett.* **2012**, *545*, 9-13.
- (50) Tulimat, L.; Mouhib, H.; Kleiner, I.; Stahl, W. The Microwave Spectrum of Allyl Acetone. *J. Mol. Spectrosc.* **2015**, *312*, 46-50.
- (51) Mouhib, H.; Stahl, W. From Cats and Blackcurrants: Structure and Dynamics of the Sulfur-Containing Cassis Odorant Cat Ketone. *Chem. Biodivers.* **2014**, *11*, 1554-1566.
- (52) Ilyushin, V. V.; Hougen, J. T. A Fitting Program for Molecules with Two Equivalent Methyl Tops and C_{2v} Point-Group Symmetry at Equilibrium: Application to Existing Microwave, Millimeter and Sub-Millimeter Wave Measurements of Acetone. *J. Mol. Spectrosc.* **2013**, *289*, 41-49.
- (53) Wilcox, D. S.; Shirar, A. J.; Williams, O. L.; Dian, B. C. Additional Conformer Observed in the Microwave Spectrum of Methyl Vinyl Ketone. *Chem. Phys. Lett.* **2011**, *508*, 10-16.
- (54) Uriarte, I.; Melandri, S.; Maris, A.; Calabrese, C.; Cocinero, E. J. Shapes, Dynamics, and Stability of β -Ionone and Its Two Mutants Evidenced by High Resolution Spectroscopy in the Gas Phase. *J. Phys. Chem. Lett.* **2018**, *9*, 1497-1502.

- (55) Lee, P. L.; Schwendeman, R. H. The Microwave Spectrum, Barrier to Internal Rotation, and Dipole Moment of Cyclopropyl Methyl Ketone. *J. Mol. Spectrosc.* **1972**, *41*, 84-94.
- (56) Van, V.; Stahl, W.; Nguyen, H.V.L. The Structure and Torsional Dynamics of Two Methyl Groups in 2-Acetyl-5-Methylfuran as Observed by Microwave Spectroscopy. *ChemPhysChem* **2016**, *17*, 3223-3228.
- (57) Tubergen, M. J.; Lavrich, R. J.; Plusquellic, D. F.; Suenram, R. D. Rotational Spectra and Conformational Structures of 1-Phenyl-2-propanol, Methamphetamine, and 1-Phenyl-2-propanone. *J. Phys. Chem. A* **2006**, *110*, 13188-13194.
- (58) Cocinero, E. J.; Basterretxea, F. J.; Écija, P.; Lesarri, A.; Fernández, J. A.; Castaño, F. Conformational Behaviour, Hydrogen Bond Competition and Intramolecular Dynamics in Vanillin Derivatives: Acetovanillone and 6-Hydroxy-3-methoxyacetophenone. *Phys. Chem. Chem. Phys.* **2011**, *13*, 13310–13318.

TOC GRAPHIC

